Caveolin-1 Expression Is Critical for Vascular Endothelial Growth Factor–Induced Ischemic Hindlimb Collateralization and Nitric Oxide–Mediated Angiogenesis

Pierre Sonveaux, Philippe Martinive, Julie DeWever, Zuzana Batova, Géraldine Daneau, Michel Pelat, Philippe Ghisdal, Vincent Grégoire, Chantal Dessy, Jean-Luc Balligand and Olivier Feron

Circ. Res. 2004;95;154-161; originally published online Jun 17, 2004;
DOI: 10.1161/01.RES.0000136344.27825.72
Circulation Research is published by the American Heart Association. 7272 Greenville Avenue, Dallas, TX 72514
 Print ISSN: 0009-7330. Online ISSN: 1524-4571

Caveolin-1 Expression Is Critical for Vascular Endothelial Growth Factor–Induced Ischemic Hindlimb Collateralization and Nitric Oxide–Mediated Angiogenesis

Pierre Sonveaux,* Philippe Martinive,* Julie DeWever, Zuzana Batova, Géraldine Daneau, Michel Pelat, Philippe Ghisdal, Vincent Grégoire, Chantal Dessy, Jean-Luc Balligand, Olivier Feron

Abstract—Nitric oxide (NO) is a powerful angiogenic mediator acting downstream of vascular endothelial growth factor (VEGF). Both the endothelial NO synthase (eNOS) and the VEGFR-2 receptor colocalize in caveolae. Because the structural protein of these signaling platforms, caveolin, also represses eNOS activity, changes in its abundance are likely to influence the angiogenic process in various ways. In this study, we used mice deficient for the caveolin-1 gene ($Cav^{-/-}$) to examine the impact of caveolae suppression in a model of adaptive angiogenesis obtained after femoral artery resection. Evaluation of the ischemic tissue perfusion and histochemical analyses revealed that contrary to $Cav^{+/+}$ mice, $Cav^{-/-}$ mice failed to recover a functional vasculature and actually lost part of the ligated limbs, thereby recapitulating the effects of the NOS inhibitor L-NAME administered to operated $Cav^{+/+}$ mice. We also isolated endothelial cells (ECs) from $Cav^{-/-}$ aorta and showed that on VEGF stimulation, NO production and endothelial tube formation were dramatically abrogated when compared with $Cav^{+/+}$ ECs. The Ser1177 eNOS phosphorylation and Thr495 dephosphorylation but also the ERK phosphorylation were similarly altered in VEGF-treated $Cav^{-/-}$ ECs. Interestingly, caveolin transfection in $Cav^{-/-}$ ECs redirected the VEGFR-2 in caveolar membranes and restored the VEGF-induced ERK and eNOS activation. However, when high levels of recombinant caveolin were reached, VEGF exposure failed to activate ERK and eNOS. These results emphasize the critical role of caveolae in ensuring the coupling between VEGFR-2 stimulation and downstream mediators of angiogenesis. This study also provides new insights to understand the paradoxical roles of caveolin (eg, repressing basal enzyme activity but facilitating activation on agonist stimulation) in cardiovascular pathophysiology. **(*Circ Res*. 2004;95:154-161.)**

Key Words: caveolin-1 ■ nitric oxide ■ vascular endothelial growth factor ■ angiogenesis ■ ischemia

Caveolae are 50- to 100-nm cell surface invaginations playing key roles in vesicular transport and signal transduction.[1] The structural protein of these plasmalemmal microdomains, caveolin, acts as a scaffold for many caveolar residents.[2] The caveolin-1 isoform is particularly abundant in endothelial cells (ECs) where it regulates various functions including transcytosis, permeability, vascular tone, and angiogenesis.[3]

Recently, Woodman et al[4] documented that in a model of tumor cell injection in caveolin-deficient mice ($Cav^{-/-}$), angiogenesis was markedly reduced in comparison with wild-type (WT) animals. Although the same authors showed that the reduction in vessel density could be reproduced in a model of Matrigel plugs supplemented with bFGF,[4] the mechanisms supporting the role of caveolin in the angiogenic response to exogenous stimuli remain poorly understood and, based on previous publications,[5–9] a matter of debate.

For instance, the well-established inhibitory interaction between caveolin and the endothelial nitric oxide (NO) synthase (eNOS)[10,11] led us and others to examine whether the modulation of this complex could impact on angiogenesis. In agreement with the proangiogenic properties of NO,[12,13] we have documented that synthetic peptides derived from the caveolin scaffolding domain (CSD) could block the NO-dependent angiogenesis in a model of ECs cultured on Matrigel.[14] Gratton and colleagues reported that the same CSD peptides could block NO-mediated vascular permeability[5] (known as an early event in the process of angiogenesis). We also reported that statins downregulated the expression of caveolin in ECs and promoted NO-dependent angiogenesis in a model of arteries cultured in Matrigel.[14]

In contrast, other groups reported that caveolin overexpression stimulated,[6] and conversely, that caveolin downregulation inhibited, tube formation.[7] Whether this was NO-dependent was, however, not discussed, and the use of superconfluent ECs made impossible the comparison with previous work integrating the overall proliferative-migratory-

Original received August 25, 2003; resubmission received January 15, 2004; revised resubmission received June 3, 2004; accepted June 7, 2004.
From the University of Louvain Medical School, Unit of Pharmacology and Therapeutics, Brussels, Belgium.
*Both authors contributed equally to this work.
Correspondence to Olivier Feron, University of Louvain Medical School, Pharmacology and Therapeutics Unit, UCL-FATH 5349, 53, Ave E. Mounier, B-1200 Brussels, Belgium. E-mail feron@mint.ucl.ac.be

Circulation Research **is available at http://www.circresaha.org** **DOI: 10.1161/01.RES.0000136344.27825.72**

differentiation process. In fact, endogenous caveolin-1 appeared to be downregulated during EC proliferation[8] but upregulated during their differentiation into tubular networks in vitro.[6]

Part of the controversy about the pro- and antiangiogenic effects of caveolin could also arise from the multiple, and sometimes opposite, roles played by caveolin and caveolae. Indeed, whereas caveolin is known to repress the catalytic activity of various enzymes, caveolae are thought to facilitate and amplify signaling cascades through the compartmentation of receptors with their effectors/mediators,[1,2] a process named "the caveolar paradox."[9] In this article, we used mice genetically deficient for caveolin-1 (Cav$^{-/-}$)[15–17] to study the balance between these apparently paradoxical roles of the caveolin platform in the context of postnatal angiogenesis. Accordingly, the role of caveolin/caveolae in the vascular endothelial growth factor (VEGF) signaling cascades (involving the caveolar and noncaveolar resident eNOS and ERK, respectively) was evaluated in the mouse model of postischemic revascularization and in cultured ECs isolated from Cav$^{-/-}$ mice and their littermate controls.

Materials and Methods

Mice and Cells

Caveolin-deficient (Cav$^{-/-}$) mice[15] (a gift from Drs M. Drab and T.V. Kurzchalia, Max Planck Institute for Molecular Cell Biology and Genetics, Dresden, Germany) and their control littermate (Cav$^{+/+}$) were generated through heterozygous matings and housed in our local facility. Each procedure was approved by the local authorities according to national animal care regulations. ECs were obtained from aorta according to the primary explant procedure, which allows to isolate limited but pure cell preparations[18] (see also the expanded Materials and Methods section provided in the online data supplement available at http://circres.ahajournals.org). ECs were transfected with either 1 or 5 μg caveolin-1 cDNA (per 35-mm dish) using the Amaxa device and recommended reagents; the transfection efficiency reached 65±7% indifferently of the amounts of plasmids, and an irrelevant plasmid encoding β-galactosidase was used as a control to maintain identical amounts of DNA in each transfection.

Ischemic Hindlimb Reperfusion Assay

Anesthetized mice underwent a double femoral artery and vein 2-mm resection under a stereoscopic microscope while innervation was carefully preserved. In one set of experiments, we also used Cav$^{+/+}$ mice receiving L-NAME (500 mg/L) in the drinking water. Blood flow in the ligated and control opposite legs was measured (before and up to 20 days after surgery) with a Laser Doppler perfusion imager (LDI, Moor Instruments). Briefly, mice were anesthetized and after local fur removal using a depilatory cream, were placed on a heating pad (37°C) to minimize temperature variations. Leg perfusion was evaluated on the basis of colored histogram pixels and normalized for the leg surface analyzed.

Immunohistochemistry and Immunoblotting

CD31 antibody and FITC-labeled *Lycopersicon esculentum* lectin staining were performed to label the vasculature in the ischemic leg and immunoblotting (IB) was performed, as previously described.[14,19]

NO Determination

The determination of NO level, eg, the 8- or 24-hour accumulation of NO derivatives in the (serum-deprived) cell-bathing medium, was performed using the Nitric Oxide Colorimetric Assay (Roche Diagnostics, Mannheim, Germany).

Angiogenesis Assays

To assess in vitro the angiogenic process, an assay of endothelial network formation (eg, plating of EC on Matrigel) was used as previously reported.[14,20] EC reorganization in capillary-like structures was observed using an inverted phase contrast microscope and the length of the endothelial network quantified by analysis of images randomly captured by a video-camera system. Because inevitable interlot differences in the composition of growth-factor-deprived Matrigel (eg, in the basal proangiogenic capability of Matrigel), the extent of the endothelial network in the different conditions tested was always compared within a same set of experiments and relative values were used for interassay comparisons.

Subcellular Fractionation

Cultured ECs (three 100-mm dishes per condition) were lysed in ice-cold TNE buffer (25 mmol/L Tris, 150 mmol/L NaCl, and 1 mmol/L EGTA) containing a cocktail of protease inhibitors (Sigma). After 10 passages through 23G and 26G needles, postnuclear supernatants were obtained after centrifugation at 800*g* at 4°C for 10 minutes. PNS was then incubated with 1% Lubrol-X at 4°C for 30 minutes under constant agitation. The solution was brought to 40% sucrose in TNE/Lubrol and, after homogenization, overlaid by a two-step sucrose gradient (30% to 10% sucrose in TNE/Lubrol). Gradients were centrifuged at 38 000 rpm for 16 to 18 hours in a SW41 rotor (Beckman Instruments Inc) at 4°C. Eight fractions (1.5 mL) plus the pellet (resuspended in 1.5 mL TNE/Lubrol) were harvested from the top. In several experiments, fractions 1 to 4 and 6 to 9 were pooled and named low-density (LD) and high-density (HD) membranes, respectively.

Statistical Analyses

Data are normalized to control condition and are presented for convenience as mean±SE. Statistical analyses were made using Student *t* test or 2-way ANOVA where appropriate.

Results

NO-Mediated Ischemic Hindlimb Reperfusion Is Defective in Cav$^{-/-}$ Mice

To address the role of caveolin in postnatal angiogenesis, we used the well-established mouse model of femoral artery/vein ligation known to induce VEGF-dependent collateral vessel development.[21,22] Figure 1A shows that after resection, a net drop in blood flow was observed in the ligated hindlimb. In wild-type Cav$^{+/+}$ mice, the difference in perfusion between the right and left hindlimbs (eg, ligated versus non-ligated, respectively) progressively decreased to be insignificant after 8 days. By contrast, in Cav$^{-/-}$ mice, the ligated hindlimb remained underperfused and would not recover (see Figure 1B). In fact, at day 21, more than 70% of the Cav$^{-/-}$ mice lost their whole leg, whereas all the Cav$^{+/+}$ mice completely recovered the use of their leg (see also online Figure 1, available in the online data supplement). To validate the critical role of NO (identified as a critical mediator of VEGF in this model),[22] we also treated Cav$^{+/+}$ mice with the NOS inhibitor L-NAME after resection. As shown in Figure 1, L-NAME administration prevented the limb reperfusion. However, the NOS inhibition exerted less profound deleterious effects than the caveolin-1 deficiency: half of L-NAME–treated mice lost toes (versus 100% of the Cav$^{-/-}$ mice) and only 15% lost their whole leg (see also online Figure 1).

The defect in collateralization in Cav$^{-/-}$ mice, suggested by the early-stage underperfusion and confirmed by the later loss of limb integrity, was further validated by histochemical

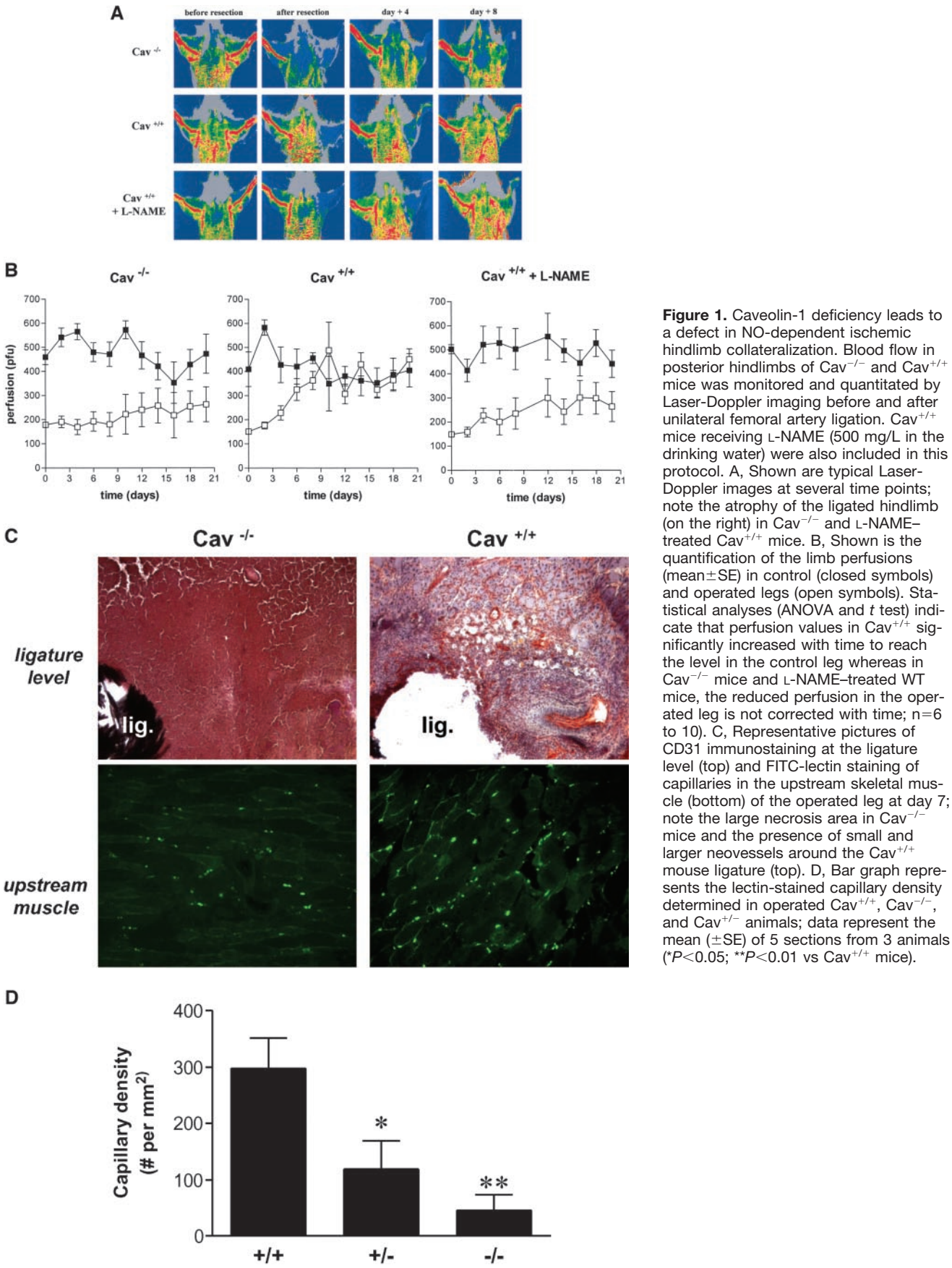

Figure 1. Caveolin-1 deficiency leads to a defect in NO-dependent ischemic hindlimb collateralization. Blood flow in posterior hindlimbs of $Cav^{-/-}$ and $Cav^{+/+}$ mice was monitored and quantitated by Laser-Doppler imaging before and after unilateral femoral artery ligation. $Cav^{+/+}$ mice receiving L-NAME (500 mg/L in the drinking water) were also included in this protocol. A, Shown are typical Laser-Doppler images at several time points; note the atrophy of the ligated hindlimb (on the right) in $Cav^{-/-}$ and L-NAME–treated $Cav^{+/+}$ mice. B, Shown is the quantification of the limb perfusions (mean±SE) in control (closed symbols) and operated legs (open symbols). Statistical analyses (ANOVA and *t* test) indicate that perfusion values in $Cav^{+/+}$ significantly increased with time to reach the level in the control leg whereas in $Cav^{-/-}$ mice and L-NAME–treated WT mice, the reduced perfusion in the operated leg is not corrected with time; n=6 to 10). C, Representative pictures of CD31 immunostaining at the ligature level (top) and FITC-lectin staining of capillaries in the upstream skeletal muscle (bottom) of the operated leg at day 7; note the large necrosis area in $Cav^{-/-}$ mice and the presence of small and larger neovessels around the $Cav^{+/+}$ mouse ligature (top). D, Bar graph represents the lectin-stained capillary density determined in operated $Cav^{+/+}$, $Cav^{-/-}$, and $Cav^{+/-}$ animals; data represent the mean (±SE) of 5 sections from 3 animals (*$P<0.05$; **$P<0.01$ vs $Cav^{+/+}$ mice).

characterizations. Figure 1C (top) shows that Cav$^{-/-}$ mice developed necrosis around the ligature whereas a strong CD31 immunostaining of large and smaller vessels was observed in Cav$^{+/+}$ mice. We also used FITC-labeled lectin (Figure 1C, bottom) and nonleaky FITC-dextran (see online Figure 2) to document the lack of functional microvasculature in Cav$^{-/-}$ mice. Quantification of lectin-staining revealed that the capillary density was 7-fold lower in Cav$^{-/-}$ mice than in Cav$^{+/+}$ mice (Figure 1D); of note, Cav$^{+/-}$ mice showed an intermediary phenotype with 3-fold less capillaries than Cav$^{+/+}$ mice (Figure 1D).

ECs Derived From Cav$^{-/-}$ Mice Reveal a Defect in VEGF-Induced NO-Mediated Angiogenesis

To evaluate the nature of the alterations in the angiogenic pathway in caveolin-deficient mice, we isolated ECs from Cav$^{-/-}$ and Cav$^{+/+}$ aorta rings (see online Figure 3) and compared their ability to form networks when seeded on growth factor-reduced Matrigel (Figure 2A). Figure 2B shows that in basal conditions, the extent of EC reorganization was not significantly different between Cav$^{-/-}$ ECs and Cav$^{+/+}$ ECs. When these experiments were repeated in the presence of VEGF (25 ng/mL), the extent of EC reorganization was dramatically higher in Cav$^{+/+}$ECs than in Cav$^{-/-}$ ECs ($P<0.01$, n=4) (Figure 2B, solid bars) and most of the proangiogenic effects observed appeared to be NO-dependent as revealed by the use of the NOS inhibitor L-NAME (Figure 2B, open bars).

The defect in the VEGF/eNOS coupling in Cav$^{-/-}$ mice was confirmed by directly measuring the amounts of NOx ($NO_2^- + NO_3^-$), which accumulated after 8 hours in the medium bathing ECs. As shown in Figure 2C, the VEGF-induced production of NOx in Cav$^{-/-}$ ECs amounted to less than 20% of the levels in wild-type (WT) ECs ($P<0.01$, n=6). By contrast, the calcium ionophore A23187 did not reveal differences in NOx production, confirming previous data documenting that the overwhelming increase in intracellular Ca^{2+} observed on A23187 stimulation was sufficient to allow Ca^{2+}-bound calmodulin to competitively displace caveolin (even overexpressed) from eNOS binding.[11,19] Of note, the basal eNOS activity was slightly higher in Cav$^{-/-}$ ECs than in WT ECs; this difference reached statistical significance ($P<0.05$, n=4) when measuring the 24-hour accumulation of NOx content in the medium (not shown).

We also tested whether the eNOS phosphorylation status, which is known to be regulated by VEGF,[19] was modified in Cav$^{-/-}$ ECs. Figure 2D reveals a dramatically different pattern of phosphorylation. Indeed, whereas VEGF induced the phosphorylation of eNOS on the serine 1177 in WT ECs (+420%, $P<0.01$, n=4), this phosphorylation was undetectable in VEGF-treated Cav$^{-/-}$ ECs. In addition, VEGF exposure led to the dephosphorylation of eNOS on the threonine 495 in WT ECs (−82%, $P<0.01$, n=4) but not in Cav$^{-/-}$ ECs ($P>0.1$, n=4).

Lack of Caveolin Alters the VEGFR-2 Receptor Compartmentation and the VEGF/ERK Signaling Pathway

Because our findings suggested an alteration in the VEGF coupling to eNOS activation, we also examined the impact of

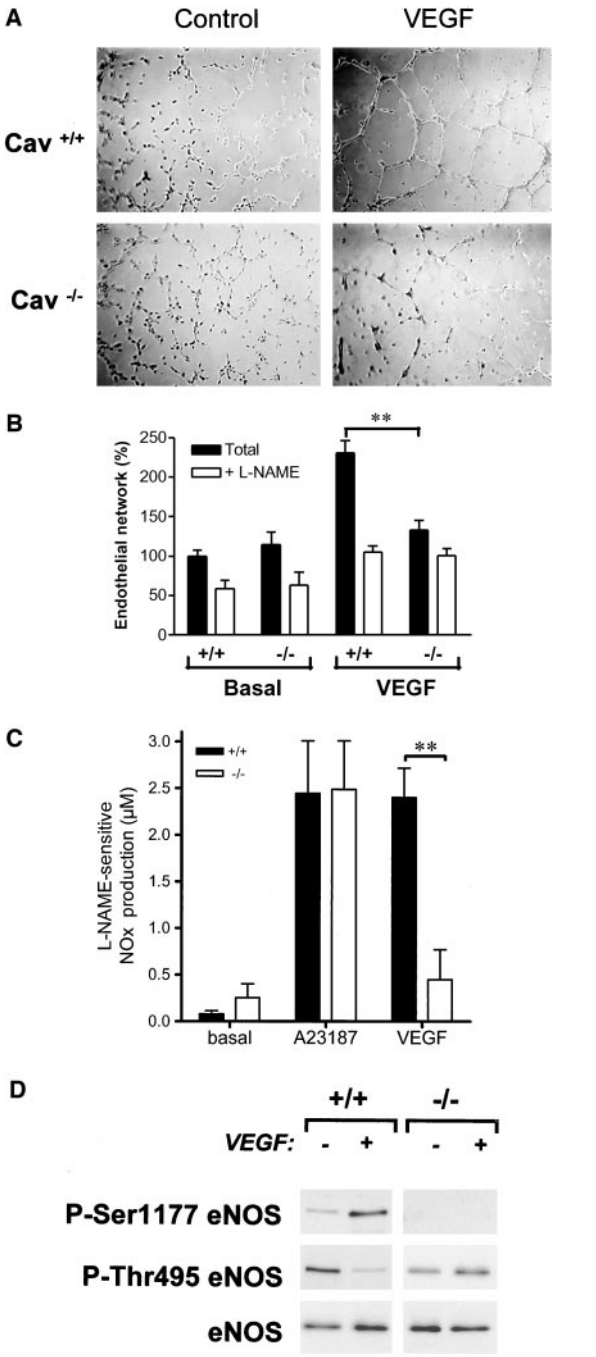

Figure 2. ECs derived from Cav$^{-/-}$ mouse reveal a defect in angiogenesis and VEGF-induced eNOS activation. A, Representative pictures of the neoformed network of Cav$^{-/-}$ and Cav$^{+/+}$ ECs cultured on Matrigel in basal conditions or on 8-hour exposure to VEGF (25 ng/mL). B, Bar graph represents the relative extents of the EC reorganization in the absence (black bars) or in the presence (open bars) of L-NAME (**$P<0.01$, n=4). The 100% value was set up as the Cav$^{+/+}$ EC network extent determined in basal conditions. C, Bar graph represents the L-NAME–sensitive NOx production (for 8 hours) by Cav$^{+/+}$ and Cav$^{-/-}$ ECs in unstimulated conditions and on exposure to 0.5 μmol/L A23187 or 25 ng/mL VEGF (**$P<0.01$, n=6); these treatments were not associated with changes in cell numbers or eNOS abundance. Of note, a residual L-NAME–insensitive NOx accumulation was observed for each condition. D, Shown are representative immunoblotting experiments with eNOS and the indicated anti–phospho-eNOS antibodies. Cav$^{-/-}$ and Cav$^{+/+}$ ECs were treated or not with 25 ng/mL VEGF for 15 minutes before lysis. Quantitative data from 4 different experiments are presented in the Results section.

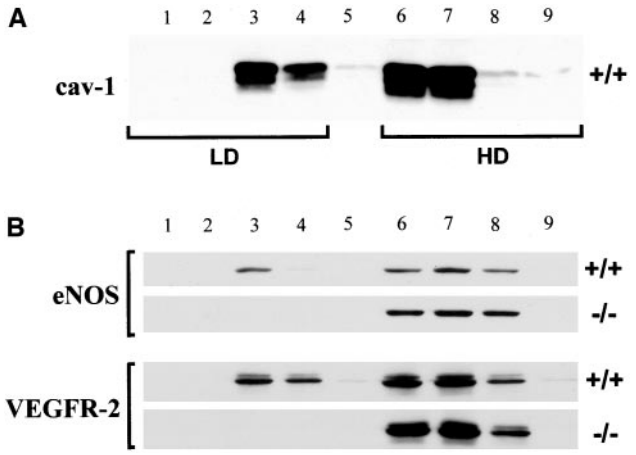

Figure 3. Caveolin-1 deficiency alters the subcellular distribution of both eNOS and VEGFR-2 in ECs. Isolated $Cav^{+/+}$ and $Cav^{-/-}$ ECs were cultured to confluence before lysis. Subcellular fractionation was then performed on sucrose gradient and the different fractions were loaded onto acrylamide gels. Shown are representative immunoblotting experiments with caveolin antibodies from $Cav^{+/+}$ ECs (A) and with VEGFR-2 and eNOS antibodies (B) from both $Cav^{+/+}$ and $Cav^{-/-}$ ECs. Densitometric analyses from 4 different experiments revealed 5.7- and 4.6-fold enrichment, respectively, in LD vs HD fractions.

the caveolin deficiency on the subcellular location of the VEGF receptor Flk-1 (VEGFR-2). We used a caveolae isolation method based on Lubrol extraction and sucrose gradient fractionation. Figure 3A shows a representative caveolin immunoblot of the different fractions obtained from WT EC lysates. Although the amounts of total proteins recovered in low-density (LD) fractions (1 to 4) amounted to 2% to 4%, we consistently found 30% to 40% of caveolin signal in those fractions, representing a 10- to 20-fold enrichment [versus the high-density (HD) fractions (6 to 9)]. Using this method, we looked at the subcellular distribution of eNOS and VEGFR-2 in $Cav^{-/-}$ and $Cav^{+/+}$ ECs. As depicted in Figure 3B, both VEGFR-2 and eNOS could be found in LD fractions of $Cav^{+/+}$ ECs, whereas in ECs isolated from $Cav^{-/-}$, both proteins were exclusively found in HD fractions. It should be emphasized that although same volumes of collected fractions were loaded on the gel, the amounts of proteins present in the LD fractions (1 to 4) only amounted to ≈3% of the proteins in the HD fractions (6 to 9). Therefore, the ≈15% of total eNOS or VEGFR-2 signals in the LD lanes (1 to 4) correspond in fact to a ≈5-fold (absolute) enrichment of these proteins in the caveolar membranes (see Figure 3 legend).

To further identify the level of the alteration in the VEGF coupling cascade, we also examined the ability of VEGF to stimulate the phosphorylation of the noncaveolar protein ERK in both $Cav^{+/+}$ and $Cav^{-/-}$ ECs. Figure 4A shows that lack of caveolin prevented the time-dependent VEGF-induced phosphorylation of ERK. Also, in the $Cav^{-/-}$ ECs, an increase in the VEGF doses only led to a weak increase in phosphorylated ERK whereas a dose-dependent increase in ERK phosphorylation was observed in VEGF-treated $Cav^{+/+}$ ECs (Figure 4B). Of note, the status of eNOS phosphorylation in $Cav^{-/-}$ ECs (as reported in Figure 2D) was not altered either by increasing the VEGF dose nor the time of exposure (not shown).

Caveolin Titration of the VEGFR-2 Coupling to Both eNOS and ERK

We then verified whether caveolin transfection could restore both the VEGF/ERK and VEGF/eNOS couplings in $Cav^{-/-}$ ECs. Figure 5A (top) shows that the transfection of $Cav^{-/-}$ ECs with low amounts of caveolin-coding plasmids led to a partial recovery of the phosphorylation of ERK by VEGF. However, at higher levels of recombinant caveolin (obtained by using 5-fold more caveolin plasmids), VEGF stimulation failed to induce the phosphorylation of ERK. A similar pattern was found for the activating eNOS phosphorylation on the serine 1177: low levels of recombinant caveolin restored the VEGF-induced Ser1177 phosphorylation, whereas higher caveolin amounts blocked this process (Figure 5A, middle lanes). Of note, even in basal condition, the low serum concentration (present in the medium after transfection) was probably already sufficient to induce Ser1177 phosphorylation. Interestingly, we also found that on VEGF stimulation, eNOS was dephosphorylated on the threonine 495 when low levels of caveolin were present but not when caveolin was absent or in the presence of higher levels of the recombinant protein (Figure 5A, middle lanes). The determination of the NOx production in transfected $Cav^{-/-}$ ECs also led to the identification of a bell-shaped pattern of NO production reflecting the stimulatory and inhibitory roles of low and high levels of recombinant caveolin, respectively, on eNOS activation by VEGF (Figure 5B, left). Figure 5B also shows that caveolin dose-dependently decreased eNOS basal activity, and that receptor-independent activation of eNOS by the calcium ionophore A23187 did not vary with the abundance of recombinant caveolin. We also found that VEGF-induced NO production in $Cav^{-/-}$ ECs transfected with low levels of caveolin and wild-type mouse $Cav^{+/+}$ ECs were in

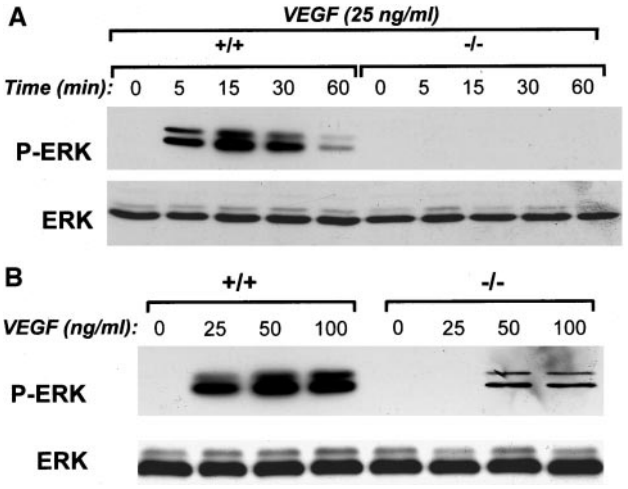

Figure 4. Caveolin-1 deficiency alters the VEGF-induced ERK activation in ECs. Isolated $Cav^{-/-}$ and $Cav^{+/+}$ ECs were treated with VEGF for increasing periods of time (A) and at increasing doses (B). Shown are representative immunoblotting experiments with phospho-ERK and ERK antibodies from $Cav^{-/-}$ and $Cav^{+/+}$ ECs. This experiment was repeated 3 times with similar results.

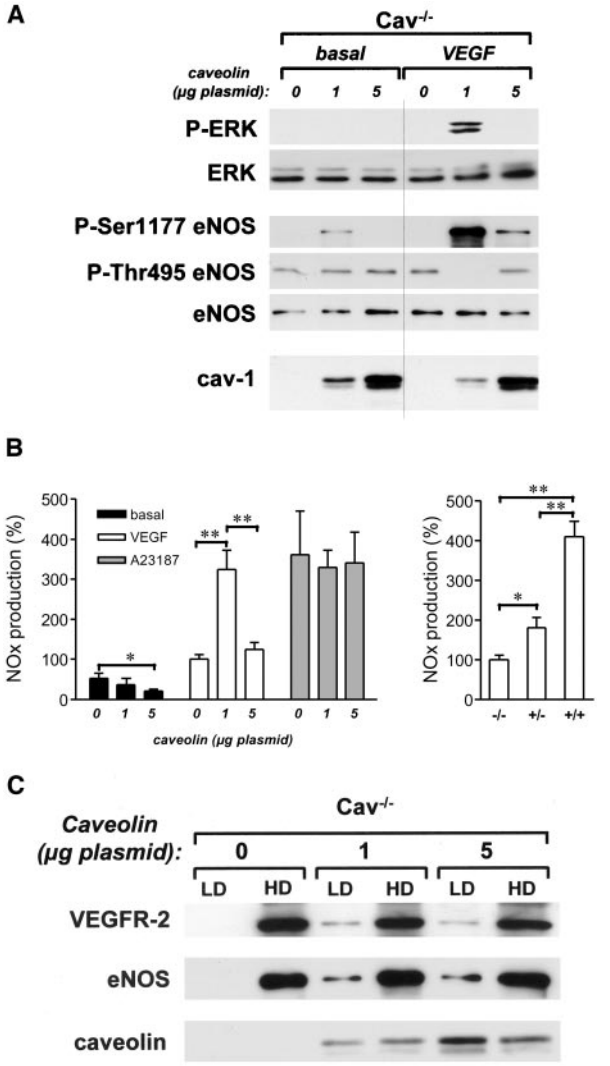

Figure 5. Caveolin knock-in experiments unravel the double role of caveolin: repressing basal activity and promoting activation. Isolated Cav$^{-/-}$ ECs were transfected with low (1 μg) or high (5 μg) amounts of caveolin plasmid; sham-transfected ECs were used as controls. A, Immunoblotting was performed to evaluate the phosphorylation status of ERK and eNOS (both on Ser1177 and Thr495) in transfected Cav$^{-/-}$ ECs in basal conditions or on VEGF exposure (50 ng/mL, 15 minutes). Abundance of ERK and eNOS as well as the level of recombinant caveolin expression were also evaluated. B, Bar graph (left) compares the amounts of NOx accumulated for 8 hours in the medium bathing Cav$^{-/-}$ ECs transfected with 0, 1, or 5 μg caveolin plasmid in basal conditions or on VEGF or A23187 exposure (*P<0.05, **P<0.01 vs no caveolin plasmid in the corresponding condition, n=3). For comparison, the VEGF-induced production of NOx (for the same period of time) in the extracellular medium of Cav$^{-/-}$, Cav$^{+/-}$, and Cav$^{+/+}$ ECs is also presented in a bar graph (right) (*P<0.05, **P<0.01 vs Cav$^{-/-}$ condition, n=3). C, Subcellular fractionation on sucrose gradient was also performed to evaluate the effect of caveolin reexpression on the distribution of the VEGFR-2 receptor and eNOS between the low-density (LD) and high-density (HD) fractions. These experiments were repeated 3 times with similar results.

the same range (compare left and right panels in Figure 5B). Interestingly also, the presence of a single allele of caveolin (Cav$^{+/-}$) was insufficient to restore normal eNOS activation (Figure 5B, right), thereby further confirming the critical role of caveolin in titrating VEGF-induced angiogenesis.

Of note, we verified by using GFP-encoding plasmid that the efficiency of the transfection (65±7%) was identical whatever the amounts of plasmids used in the electroporation. Importantly, this indicated that in our knock-in experiments, the amounts of recombinant caveolin detected by immunoblotting (Figure 5A, last lane) represented the relative amounts of caveolin expressed in two-thirds of the EC monolayers. In both conditions (eg, low and high amounts of transfected plasmids), the expression of both the VEGFR-2 receptor and eNOS was recovered in LD fractions to the same extents (see Figure 5C). Also, as previously observed in Cav$^{+/+}$ ECs (not shown), caveolin transfection of Cav$^{-/-}$ ECs did not lead to ERK targeting in LD membranes, confirming the absence of caveolar compartmentation of the kinase with the VEGFR-2 in basal conditions.

Discussion

Caveolin is a well-established endogenous inhibitory protein modulating the activity of various enzymes through direct interactions.[2] In most cases, a dynamic equilibrium responding to the mass action law was documented to regulate the interactions of caveolin with its multiple partners.[2] Accordingly, increase in the abundance of caveolin leads to a decrease in basal activity of eNOS[23] and ERK.[24] In the present study, we showed that on agonist stimulation, this inhibitory role of caveolin is confounded by its role as a structural protein for the constitution of caveolae. Indeed, we found that in a model of VEGF/NO-mediated angiogenesis,[21,22,25] the lack of caveolin, instead of boosting the process because of the brake removal, led to a dramatic defect in postischemic neovessel formation.

That the defects in eNOS activation on VEGF stimulation were involved in the inability of Cav$^{-/-}$ mice to stimulate angiogenesis was further validated by using ECs isolated from these mice, eg, (1) the ability of Cav$^{-/-}$ ECs to form tubes on Matrigel on VEGF stimulation was dramatically repressed when compared with Cav$^{+/+}$ ECs; in the latter cells, the NOS inhibitor L-NAME prevented the VEGF-induced endothelial networking; (2) the VEGF-induced NO production was dramatically inhibited in Cav$^{-/-}$ ECs, whereas the unspecific eNOS stimulation by the calcium ionophore led to similar amounts of NO release; and (3) the VEGF-induced phosphorylation of eNOS on Ser1177 and dephosphorylation on Thr495, both considered as hallmarks of eNOS activation, were abrogated in Cav$^{-/-}$ ECs but not in Cav$^{+/+}$ ECs.

Whether this defect in the VEGF/NO-mediated angiogenic pathway accounts for the previously reported reduction in vessel density in tumor-bearing Cav$^{-/-}$ mice[4] requires further studies. However, the observation by the same authors that neovessel infiltration in bFGF-supplemented Matrigel was also altered in Cav$^{-/-}$ mice[4] suggests that caveolin may impact on various angiogenic signaling molecules.

In the present study, because the alterations in limb perfusion and recovery appeared even worse in Cav$^{-/-}$ mouse than in L-NAME–treated Cav$^{+/+}$, we also examined whether the VEGF binding to its receptor VEGFR-2 (eg, the receptor mediating most of the VEGF-induced angiogenic effects) was somehow altered. Induction of VEGF, as authenticated by a 4-fold increase in serum 48 hours after ligature (not shown),

was similar in $Cav^{-/-}$ mice (versus $Cav^{+/+}$ mice). By contrast, we found that although the absolute amounts of VEGFR-2 were not altered, a significant amount of this receptor normally located in low-density caveolin-enriched membranes was recovered in high-density membranes in $Cav^{-/-}$ ECs. Altogether, these findings confirmed the existence of a specific signaling platform optimizing the VEGFR-2 coupling to eNOS in wild-type cells. The absence of compartmentation of VEGFR-2 and eNOS in $Cav^{-/-}$ ECs is therefore likely to account for the defect in angiogenesis. Still, to dissociate the effects due to eNOS mislocalization from those attributable to VEGFR-2 uncoupling (because of the receptor mislocalization per se), we examined whether ERK, another downstream mediator of VEGF action (but not located in caveolae) was also altered.

Accordingly, we showed that $Cav^{+/+}$ EC exposure to VEGF rapidly led to ERK phosphorylation but that such phosphorylation was completely abrogated in $Cav^{-/-}$ ECs. Interestingly, the expression of low levels of recombinant caveolin-1 in $Cav^{-/-}$ ECs restored both the VEGFR-2 expression in low-density caveolin-enriched membranes and the ERK phosphorylation. However, when higher levels of caveolin were expressed, the restoration of VEGF-induced ERK phosphorylation was lost. This mode of regulation was extended to the VEGF/NO signaling pathway because we could similarly restore VEGF-induced changes in the eNOS phosphorylation status as well as NO production by reexpressing caveolin in $Cav^{-/-}$ ECs. Again, this was restricted to low amounts of caveolin because high expression levels of recombinant caveolin led to a tonic inhibition of the VEGF-stimulated eNOS activation. Interestingly, these data are in good agreement with the observed reduced angiogenic response to VEGF in transgenic mice overexpressing caveolin-1 in the endothelium.[26]

Beyond the biochemical demonstration of the exquisite modulation of both eNOS and ERK activity by caveolin, these data emphasize the complexity of the regulation of the multiple pathways supported by these proteins in ECs. Although ECs completely deprived of caveolae is an extreme condition very unlikely to be reached in any cardiovascular diseases, the 50% reduction in caveolin abundance in $Cav^{+/-}$ animals and the associated functional alterations (see Figures 1D and 5B) make our findings particularly relevant in the context of previous studies. Indeed, important changes in the absolute or subcellular expression levels of caveolin-1 and -3 have been reported in hypertension,[27,28] hypercholesterolemia,[23,29–32] and cardiomyopathies.[33–38] In several of these studies, a decrease in caveolin abundance[27,33] (or its translocation from caveolae)[30,35] was documented in situations of endothelial/cardiac dysfunction mostly attributable to a decrease in NO bioavailability. In others, the upregulation of caveolin[34,35] (or its translocation to caveolae)[38] was associated with beneficial compensatory/remodelling mechanisms likely to be due to an increase in NO production. In both situations, the "inhibitory" hypothesis (eg, inhibition proportional to caveolin levels) does not fit with the observed modulation of eNOS activation. Instead, the "compartmentalizing" effect of caveolin may account for the direct relationship between caveolin abundance and NO production, eg, receptor/effector coupling is either prevented or promoted when/where caveolin is downregulated or upregulated, respectively. This latter hypothesis is further supported by the presence in caveolae of receptors known to mediate NO signaling including tyrosine kinase receptors like VEGFR-2[39] but also the G protein–coupled receptors.[2]

In conclusion, although our biochemical dissection of the VEGF-dependent signaling pathway derived mostly from primary cultures of aortic ECs (which do not exactly reflect the phenotype of the EC involved in the revascularization process of the ligatured limb), this study provides some new clues to understand the physiopathology associated to changes in caveolin abundance and/or subcellular location in ECs and myocytes. Importantly, the use of mice deficient in the caveolin-1 gene allowed us to give credential to the concept identified as the "caveolar paradox"[9] (ie, caveolin can both block enzyme activity in basal condition and promote its stimulation on agonist stimulation). Obviously, important questions remain open, such as, what are the relative contributions of eNOS, ERK, and probably other enzymes (the activity of which being dependent on caveolin abundance) in in vivo angiogenesis. Also, why such signaling disturbances, including those regulated by VEGF, are not lethal. Whether the noncaveolar proportion of VEGFR-2 is involved in the regulation of other vital signaling pathways (including embryonic angiogenesis) needs certainly to be examined in the future. Still, our findings teach us that in the context of postnatal angiogenesis and cardiovascular diseases, the compartmentation paradigm should be integrated to optimize the action of drugs aiming to modulate caveolin-driven processes including collateralization, cardiac contractility, and vessel permeability and relaxation.

Acknowledgments

This work was supported by grants from the Fonds de la Recherche Scientifique Médicale. C.D. and O.F. are FNRS Research Associates. P.S. is FNRS Research Assistant. Z.B. is a visiting scientist from the Comenius University (Bratislava, Slovak Republic).

References

1. Deurs B, Roepstorff K, Hommelgaard AM, Sandvig K. Caveolae: anchored, multifunctional platforms in the lipid ocean. *Trends Cell Biol*. 2003;13:92–100.
2. Razani B, Woodman SE, Lisanti MP. Caveolae: from cell biology to animal physiology. *Pharmacol Rev*. 2002;54:431–467.
3. Frank PG, Woodman SE, Park DS, Lisanti MP. Caveolin, caveolae, and endothelial cell function. *Arterioscler Thromb Vasc Biol*. 2003;23:1161–1168.
4. Woodman SE, Ashton AW, Schubert W, Lee H, Williams TM, Medina FA, Wyckoff JB, Combs TP, Lisanti MP. Caveolin-1 knockout mice show an impaired angiogenic response to exogenous stimuli. *Am J Pathol*. 2003;162:2059–2068.
5. Gratton JP, Lin MI, Yu J, Weiss ED, Jiang ZL, Fairchild TA, Iwakiri Y, Groszmann R, Claffey KP, Cheng YC, Sessa WC. Selective inhibition of tumor microvascular permeability by cavtratin blocks tumor progression in mice. *Cancer Cell*. 2003;4:31–39.
6. Liu J, Wang XB, Park DS, Lisanti MP. Caveolin-1 expression enhances endothelial capillary tubule formation. *J Biol Chem*. 2002;277:10661–10668.
7. Griffoni C, Spisni E, Santi S, Riccio M, Guarnieri T, Tomasi V. Knockdown of caveolin-1 by antisense oligonucleotides impairs angiogenesis in vitro and in vivo. *Biochem Biophys Res Commun*. 2000;276:756–761.
8. Liu J, Razani B, Tang S, Terman BI, Ware JA, Lisanti MP. Angiogenesis activators and inhibitors differentially regulate caveolin-1 expression and

caveolae formation in vascular endothelial cells: angiogenesis inhibitors block vascular endothelial growth factor-induced down-regulation of caveolin-1. *J Biol Chem*. 1999;274:15781–15785.
9. Feron O, Kelly RA. The caveolar paradox: suppressing, inducing, and terminating eNOS signaling. *Circ Res*. 2001;88:129–131.
10. Feron O, Belhassen L, Kobzik L, Smith TW, Kelly RA, Michel T. Endothelial nitric oxide synthase targeting to caveolae. Specific interactions with caveolin isoforms in cardiac myocytes and endothelial cells. *J Biol Chem*. 1996;271:22810–22814.
11. Feron O, Saldana F, Michel JB, Michel T. The endothelial nitric-oxide synthase-caveolin regulatory cycle. *J Biol Chem*. 1998;273:3125–3128.
12. Papapetropoulos A, Garcia-Cardena G, Madri JA, Sessa WC. Nitric oxide production contributes to the angiogenic properties of vascular endothelial growth factor in human endothelial cells. *J Clin Invest*. 1997;100:3131–3139.
13. Murohara T, Horowitz JR, Silver M, Tsurumi Y, Chen D, Sullivan A, Isner JM. Vascular endothelial growth factor/vascular permeability factor enhances vascular permeability via nitric oxide and prostacyclin. *Circulation*. 1998;97:99–107.
14. Brouet A, Sonveaux P, Dessy C, Moniotte S, Balligand JL, Feron O. Hsp90 and caveolin are key targets for the proangiogenic nitric oxide-mediated effects of statins. *Circ Res*. 2001;89:866–873.
15. Drab M, Verkade P, Elger M, Kasper M, Lohn M, Lauterbach B, Menne J, Lindschau C, Mende F, Luft FC, Schedl A, Haller H, Kurzchalia TV. Loss of caveolae, vascular dysfunction, and pulmonary defects in caveolin-1 gene-disrupted mice. *Science*. 2001;293:2449–2452.
16. Razani B, Engelman JA, Wang XB, Schubert W, Zhang XL, Marks CB, Macaluso F, Russell RG, Li M, Pestell RG, Di Vizio D, Hou H, Jr., Kneitz B, Lagaud G, Christ GJ, Edelmann W, Lisanti MP. Caveolin-1 null mice are viable but show evidence of hyperproliferative and vascular abnormalities. *J Biol Chem*. 2001;276:38121–38138.
17. Zhao YY, Liu Y, Stan RV, Fan L, Gu Y, Dalton N, Chu PH, Peterson K, Ross J Jr, Chien KR. Defects in caveolin-1 cause dilated cardiomyopathy and pulmonary hypertension in knockout mice. *Proc Natl Acad Sci U S A*. 2002;99:11375–11380.
18. Nicosia RF, Villaschi S, Smith M. Isolation and characterization of vasoformative endothelial cells from the rat aorta. *In Vitro Cell Dev Biol Anim*. 1994;30A:394–399.
19. Brouet A, Sonveaux P, Dessy C, Balligand JL, Feron O. Hsp90 ensures the transition from the early Ca^{2+}-dependent to the late phosphorylation-dependent activation of the endothelial nitric-oxide synthase in vascular endothelial growth factor-exposed endothelial cells. *J Biol Chem*. 2001;276:32663–32669.
20. Sonveaux P, Brouet A, Havaux X, Gregoire V, Dessy C, Balligand JL, Feron O. Irradiation-induced angiogenesis through the up-regulation of the nitric oxide pathway: implications for tumor radiotherapy. *Cancer Res*. 2003;63:1012–1019.
21. Couffinhal T, Silver M, Zheng LP, Kearney M, Witzenbichler B, Isner JM. Mouse model of angiogenesis. *Am J Pathol*. 1998;152:1667–1679.
22. Rivard A, Fabre JE, Silver M, Chen D, Murohara T, Kearney M, Magner M, Asahara T, Isner JM. Age-dependent impairment of angiogenesis. *Circulation*. 1999;99:111–120.
23. Feron O, Dessy C, Moniotte S, Desager JP, Balligand JL. Hypercholesterolemia decreases nitric oxide production by promoting the interaction of caveolin and endothelial nitric oxide synthase. *J Clin Invest*. 1999;103:897–905.
24. Engelman JA, Chu C, Lin A, Jo H, Ikezu T, Okamoto T, Kohtz DS, Lisanti MP. Caveolin-mediated regulation of signaling along the p42/44 MAP kinase cascade in vivo: a role for the caveolin-scaffolding domain. *FEBS Lett*. 1998;428:205–211.
25. Murohara T, Asahara T, Silver M, Bauters C, Masuda H, Kalka C, Kearney M, Chen D, Symes JF, Fishman MC, Huang PL, Isner JM. Nitric oxide synthase modulates angiogenesis in response to tissue ischemia. *J Clin Invest*. 1998;101:2567–2578.
26. Bauer PM, Yu J, Chen Y, Hickey RP, Huang Y, Giordano FJ, Sessa WC. Endothelial-specific overexpression of caveolin-1 in mice reveals multiple vascular phenotypes. *Circulation*. 2003;108:1197.
27. Piech A, Dessy C, Havaux X, Feron O, Balligand JL. Differential regulation of nitric oxide synthases and their allosteric regulators in heart and vessels of hypertensive rats. *Cardiovasc Res*. 2003;57:456–467.
28. Hillman N, Cox S, Noble AR, Gallagher PJ. Increased numbers of caveolae in retinal endothelium and pericytes in hypertensive diabetic rats. *Eye*. 2001;15:319–325.
29. Zhu Y, Liao HL, Wang N, Yuan Y, Ma KS, Verna L, Stemerman MB. Lipoprotein promotes caveolin-1 and Ras translocation to caveolae: role of cholesterol in endothelial signaling. *Arterioscler Thromb Vasc Biol*. 2000;20:2465–2470.
30. Blair A, Shaul PW, Yuhanna IS, Conrad PA, Smart EJ. Oxidized low density lipoprotein displaces endothelial nitric-oxide synthase (eNOS) from plasmalemmal caveolae and impairs eNOS activation. *J Biol Chem*. 1999;274:32512–32519.
31. Peterson TE, Poppa V, Ueba H, Wu A, Yan C, Berk BC. Opposing effects of reactive oxygen species and cholesterol on endothelial nitric oxide synthase and endothelial cell caveolae. *Circ Res*. 1999;85:29–37.
32. Pelat M, Dessy C, Massion P, Desager JP, Feron O, Balligand JL. Rosuvastatin decreases caveolin-1 and improves nitric oxide-dependent heart rate and blood pressure variability in apolipoprotein E$^{-/-}$ mice in vivo. *Circulation*. 2003;107:2480–2486.
33. Piech A, Massart PE, Dessy C, Feron O, Havaux X, Morel N, Vanoverschelde JL, Donckier J, Balligand JL. Decreased expression of myocardial eNOS and caveolin in dogs with hypertrophic cardiomyopathy. *Am J Physiol Heart Circ Physiol*. 2002;282:H219–H231.
34. Hare JM, Lofthouse RA, Juang GJ, Colman L, Ricker KM, Kim B, Senzaki H, Cao S, Tunin RS, Kass DA. Contribution of caveolin protein abundance to augmented nitric oxide signaling in conscious dogs with pacing-induced heart failure. *Circ Res*. 2000;86:1085–1092.
35. Ratajczak P, Damy T, Heymes C, Oliviero P, Marotte F, Robidel E, Sercombe R, Boczkowski J, Rappaport L, Samuel JL. Caveolin-1 and -3 dissociations from caveolae to cytosol in the heart during aging and after myocardial infarction in rat. *Cardiovasc Res*. 2003;57:358–369.
36. Oka N, Asai K, Kudej RK, Edwards JG, Toya Y, Schwencke C, Vatner DE, Vatner SF, Ishikawa Y. Downregulation of caveolin by chronic beta-adrenergic receptor stimulation in mice. *Am J Physiol*. 1997;273:C1957–C1962.
37. Fujita T, Toya Y, Iwatsubo K, Onda T, Kimura K, Umemura S, Ishikawa Y. Accumulation of molecules involved in alpha1-adrenergic signal within caveolae: caveolin expression and the development of cardiac hypertrophy. *Cardiovasc Res*. 2001;51:709–716.
38. Uray IP, Connelly JH, Frazier OH, Taegtmeyer H, Davies PJ. Mechanical unloading increases caveolin expression in the failing human heart. *Cardiovasc Res*. 2003;59:57–66.
39. Labrecque L, Royal I, Surprenant DS, Patterson C, Gingras D, Beliveau R. Regulation of vascular endothelial growth factor receptor-2 activity by caveolin-1 and plasma membrane cholesterol. *Mol Biol Cell*. 2003;14:334–347.

Materials and Methods.

Endothelial cell isolation. Endothelial cells (EC) were obtained from aorta according to the primary explant procedure which allows to isolate limited but pure cell preparations. Briefly, excised aorta were freed of the surrounding connective tissue under a stereomicroscope and cross-sectioned to obtain 1-mm rings. The explants were rinsed and placed on gelatin-coated surfaces for 60 hours in EGM medium (Clonetics) to generate endothelial outgrowths within the area delimited by the ring. When removing the explant, fibroblast contamination was prevented by scrapping the few cells adhering outside the ring. From the trypsinization of cells outgrown from ~15 rings isolated from one single aorta, we obtained enough cells to cover (after additional 72-96 hours) the surface of a well from a 12-well dish (eg, 4 cm^2). These passage-1 cells were then subcultured twice at 1:4 split ratio and led to the collection of a cell monolayer covering 90% of a 100-mm plate at passage 3. Confluent EC monolayers exhibited the typical cobblestone pattern and positive staining for von Willebrand factor and uptake of Di-I-Ac-LDL (fluorescence microscopy).

Immunohistochemistry and vasculature staining. Tissue samples (collected at the level of the original ligature) were cryosliced and probed with a rat monoclonal antibody against CD31 (Pharmingen). Endogenous peroxidase was inhibited by 0.3% H_2O_2 in PBS and Envision system (Dako) was used for revelation. Sections were finally counterstained with Mayer's hematoxylin. In some experiments, mice were injected through the tail vein with FITC-labeled *Lycopersicon esculentum* lectin (Vector Laboratories) in order to label the functional vasculature in the skeletal muscle above the ligature. Two minutes later, after sternotomy, a direct intraventricular bolus of fixative (1% paraformaldehyde in

PBS) was injected with a 22-G catheter. Alternatively, mice were injected FITC-conjugated dextran (MW = 500; Sigma). In all cases, cryoslices of collected tissues were examined with a Zeiss Axioskop microscope equipped for fluorescence.

Immunoblotting. Immunoblotting (IB) was carried out with antibodies directed against eNOS, ERK-1, caveolin-1 (Beckton Dickinson) and VEGFR-2 (Santa Cruz), and with phospho-specific antibodies against phospho-Ser1177 eNOS, phospho-Thr495 eNOS and phospho-Thr202/Tyr204 ERK-1/2 (NEB Cell Signaling Technologies and Upstate).

Online Supplement Figures.

Online Supplement Figure 1. Representative pictures of the anatomical damages in $Cav^{-/-}$ mice and L-NAME-treated $Cav^{+/+}$ mice at day 20 post-operation. Note the more dramatic lesions in the former (leg atrophy) than in the latter (loss of toes) as well as the absence of limb atrophy in control $Cav^{+/+}$ mice.

Online Supplement Figure 2. Typical labeling by FITC-dextran of the functional microvasculature of the operated leg at day 7; note the complete absence of specific signals in $Cav^{-/-}$ mice.

Online Supplement Figure 3. Photomicrograph of endothelial cells cultured from $Cav^{-/-}$ mouse rat aorta ring.

Online Supplement Figure 1.

Online Supplement Figure 2.

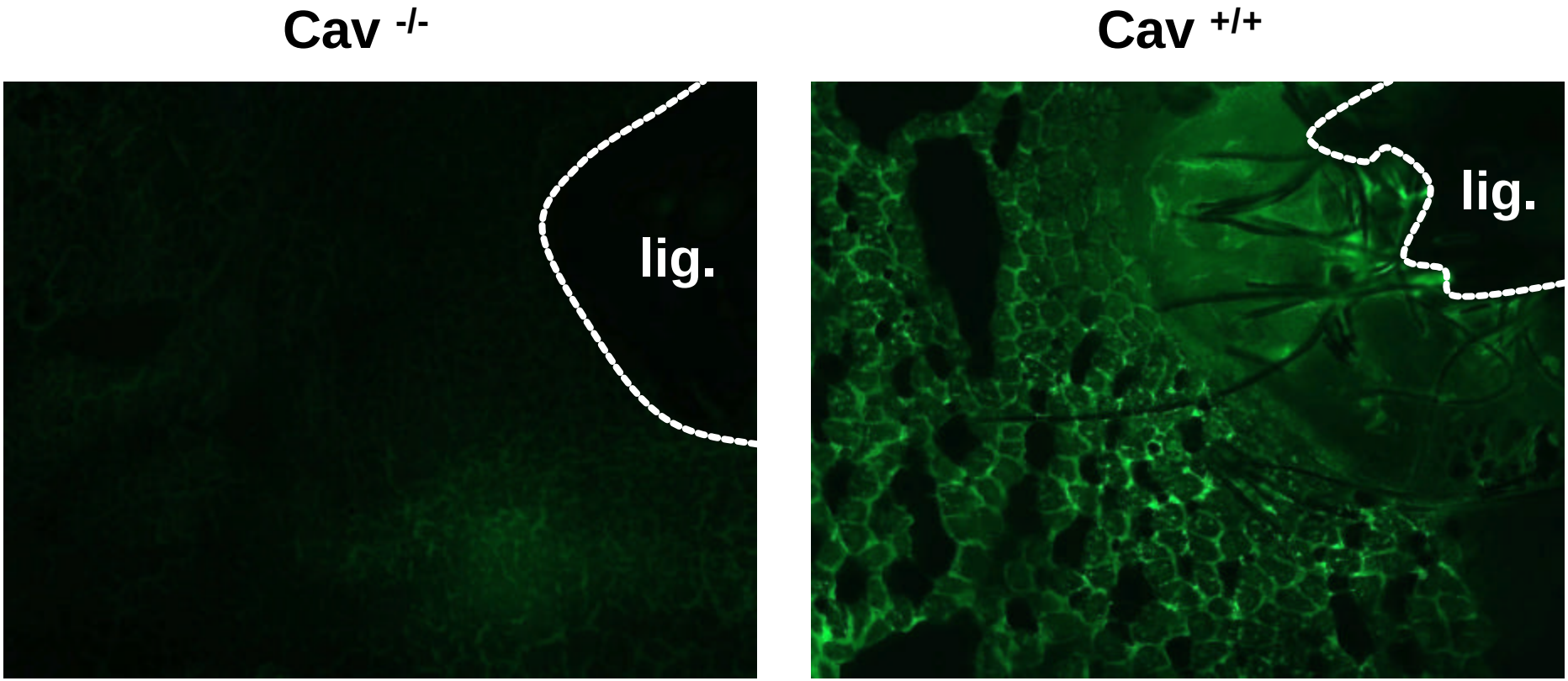

Online Supplement Figure 3.